Overview of the development of new Pt-based alloys for high temperature application in aggressive environments

by L.A. Cornish*†‡, R. Süss*†‡, R. Völkl∞, M. Wenderoth∞, S. Vorberg§, B. Fischer§, U. Glatzel∞, A. Douglas*†, L.H. Chown*†, T. Murakumo**, J. Preussner∞, D. Lupton††, L. Glaner*†‡, N.B. Maledi†‡, J.H. Potgieter†‡, M. Sephton†, and G. Williams*

Transaction Paper

Synopsis

Pt-based alloys are being developed for high temperature applications in aggressive environments, with the aim to replace the currently used nickel-based superalloys (NBSAs) in at least some of the applications where higher density is less important. The Pt-based alloys have a similar structure to the NBSAs, and since Pt is more chemically inert and has a higher melting point, the Pt-based alloys can potentially be used at higher temperatures. Room temperature tensile tests were performed and results were variable, mainly due to microstructural differences. The alloy hardnesses were in the order of 300–350HV with ultimate tensile strengths of ~800 MPa and elongations of less than 10%. These results are comparable to other alloys used at high temperatures, Transmission electron microscopy (TEM) was done at NIMS, Japan, to investigate the changes in the microstructure of Pt-Al and Pt-Al-Ir alloys at elevated temperatures using *in situ* heating up to 1100°C.

Starting from a promising Pt-Al-Cr alloy, the influence of Ni additions was investigated. After ageing finely dispersed precipitates are observed. Nb, Ta, Ti and Re increased the strength when added as a partial substitute for Al. Minor additions of B increased the creep resistance and rupture time remarkably, owing to strengthening of the grain boundaries. The evolution of the alloy development programme is presented, as well as selected properties of the multi-component Pt-base alloys.

High temperature hot corrosion (HTHC) tests were conducted at 950°C for 540 hours. Analysis of the corrosion products was conducted using a Raman spectrometer, scanning electron microscopy (SEM) with energy dispersive X-ray spectroscopy (EDS), and X-ray diffraction (XRD). Pt-based alloys displayed far superior corrosion properties compared to coated and uncoated benchmark Ni-based superalloys.

Keywords: platinum, superalloys, hardness, tensile, creep, nickel, corrosion

Introduction

Since many pieces of equipment are run at high temperatures or in aggressive chemical environments, there is a need for materials that can withstand extreme thermal, mechanical and chemical conditions for these applications. Pt-alloys are recognized for their high melting points, thermal stability and thermal shock resistance, as well as good corrosion and oxidation resistance. For several applications, the good electrical and thermal conductivity of Pt are utilized. In terms of mechanical properties, Pt-alloys are face centred cubic (fcc) in structure and so combine high ductility with high creep strength. These properties allow Pt-alloys to have potential for applications in the chemical, space technology and glass industries[1–3]. For example, in the spacecraft industry Pt-materials are used to increase the heat resistance of rocket engine nozzles. The fabrication of high-purity optical glasses and glass fibres requires the use of tank furnaces, stirrers and feeders made of a material which can withstand high temperatures, mechanical loads and corrosive attack; this is platinum. Glasses of outstanding purity, homogeneity and without bubbles can be achieved, only with platinum being used. In ceramic melting vessels, the action of stirring promotes the loosening of ceramic particles by erosion, resulting in contamination of the glass melts and thus deterioration of their optical properties, such as transmittance. For the

* *Advanced Materials Division, Mintek, South Africa.*

† *DST/NRF Centre of Excellence in Strong Materials, Johannesburg, South Africa.*

‡ *School of Chemical and Metallurgical Engineering, University of the Witwatersrand, Johannesburg, South Africa.*

∞ *University Bayreuth, Bayreuth, Germany.*

§ *FH-Jena-University of Applied Sciences Jena, Jena, Germany.*

** *National Institute of Materials Science, Tsukuba, Japan.*

†† *W.C. Heraeus GmbH, Hanau, Germany.*

 SA ISSN 0038–223X/3.00 + 0.00. Paper received Jun. 2007; revised paper received Oct. 2007.

fabrication of high quality technical glass, Pt-materials are used for many important components in combination with refractory melting furnaces, e.g. feeder systems (stirrer, stirrer cell, plunger, plunger cell, feeder, orifice), bubblers, drain bushings and thermocouple thimbles. Furthermore, technical glass fibres are drawn through bushings, which are made from Pt-alloys[1].

While pure Pt has low mechanical strength at high temperatures, alloying with Ir or Rh strongly increases the stress rupture strength[4,5]. Additionally, these solid solution strengthened alloys have good ductility at high temperatures and can also be welded. However, due to evaporation of oxides during annealing above 1100°C in air, Pt-Ir alloys have relatively high mass loss. In contrast, the alloys Pt-10%Rh and Pt-20%Rh have a very low evaporation rate, but grain coarsening of these solid solution strengthened alloys leads to a loss of properties and can result in premature failure of components.

For this reason, oxide dispersion strengthened (ODS) Pt-based alloys with improved high-temperature properties were developed[6] with small amounts of zirconium or yttrium oxides being finely distributed in the Pt matrix. By reducing dislocation mobility and stabilizing the grain boundaries, these thermally stable oxides lead to an increase of stress-rupture strength up to about 1600°C. Conventional Pt-ODS alloys are manufactured by complicated, expensive and proprietary powder metallurgical (PM) processes[7–11].

However, these alloys show excessive brittleness and susceptibility to cracking, and the low ductility does not allow these materials to withstand the stress concentrations caused by thermal expansion during frequent rapid temperature changes. Furthermore, difficulties in fabrication, in particular a decrease in strength due to coagulation the oxide particles after welding, have discouraged the full potential of the ODS platinum alloys[1].

W.C. Heraeus produces ODS Pt-alloys, the Pt DPH® alloys, in a melting process with subsequent internal oxidation, avoiding the disadvantages mentioned above. Thus, these Pt DPH alloys show good ductility, with oxidation and corrosion resistance comparable to solid solution strengthened Pt-alloys[12].

Another new group of Pt-alloys, the so-called Pt-based superalloys[13–18] possess even higher strength than solid solution and dispersion strengthened Pt-alloys at temperatures up to 1300°C. Since Pt is more chemically inert and has a higher melting point (1769°C as opposed to 1455°C), Pt-based alloys can be used at higher temperatures than most of the NBSAs[19]. In these materials, strengthening is achieved by the precipitation strengthening mechanism, which is simliar to that in Ni-based superalloys. Hill and co-workers[20,21] conducted an extensive assessment of systems with Pt as major constituent based on: high phase stability, high melting point, oxidation and hot corrosion resistance, high thermal conductivity, and low thermal expansion. It would have been preferable also to have selected for low density, but since platinum was the major constituent, this was not possible. The alloys based on Pt-Al exhibited the highest potential, not only because of possible precipitation strengthening of Pt_3Al, but also due to high oxidation resistance. However, it must be remembered that in the Pt-Al system, the high temperature cubic $L1_2$ Pt_3Al phase transforms to a tetragonal structure at lower temperatures[22,23], although it was believed that the beneficial high temperature phase could be stabilized by alloying additions. If this could be achieved, then similar $\gamma+\gamma'$ structures to those in Ni-base superalloys would give similar properties.

The microstructure is of prime importance because the NBSAs derive their excellent properties from a very fine dispersion of precipitates based on Ni_3Al in a Ni-rich matrix. The particles are ordered, and apart from the ordering, their structure and lattice dimensions are effectively the same as the matrix: face centred cubic (fcc)[24], which gives a very low surface energy between the two phases, and thus a very limited driving force to reduce the surface area, which stabilizes the precipitates against coarsening.

Although a higher strength would likely to be obtained from a higher misfit, there has to be a compromise between coarsening rate and strength, because the particles with higher misfit would have more energy for coarsening, and thus would be less stable at high temperatures. It could be argued that where cost is of lesser importance (i.e. in the military), a high misfit for higher strength but a shorter life from coarsening is preferred, whereas for land-based turbines, the opposite may be adopted).

Thus, the two-phase structure is very stable at high temperatures, and the precipitates keep their cuboid form. The stability is beneficial because it means that there is more interface area for the dislocations to interact with, which slows the dislocation movement down, thereby strengthening the alloys. Since the ~Ni_3Al phase is an ordered fcc phase, $L1_2$, this means that any dislocations from the disordered fcc matrix need to dissociate into partial dislocations before they can pass into the precipitates. The splitting of the matrix dislocations has to occur on entry to the precipitates so that like atoms are not brought together. Although the splitting takes energy, it is still much less than that for an undissociated dislocation to enter the precipitate[25].

The Pt-based alloys were designed to mimic the microstructure of the NBSAs, as closely as possible. However, there is a potential problem in that whereas there is only one structure for Ni_3Al, there are at least two, and possibly three for Pt_3Al. The highest temperature Pt_3Al structure is cubic and is the most favourable[22,23]; the lower temperature structures are tetragonal[22,23], and any transformations between the structures could be deleterious. Thus, one of the major roles for alloying elements is to stabilize the high temperature near-cubic Pt_3Al phase. Apart from the stabilization of cubic ($L1_2$) Pt_3Al, additional elements were added to improve the strengthening, oxidation resistance and formability of the alloys. The Pt-based alloys have been studied in terms of microstructure, oxidation resistance, creep and tensile strength, and they have shown great promise.

Previous work

The work has started at Mintek, initiated from discussion with NIMS workers in Japan on their Ir- and Rh-containing alloys[26,27]. Work is also ongoing based at Bayreuth

Overview of the development of new Pt-based alloys

University and Fachhochschule Jena in Germany, and there are also co-workers at Leeds and Oxford universities in the UK. Locally, the work has been done under the auspices of the Platinum Development Initiative (PDI). This initiative was officially started in April 1997 with the aim of encouraging new research into platinum-based alloys that would eventually lead to an increased off-take for platinum. Another hope was that further research would be encourages following publication of the PDI's research, and the world network of Pt researchers would grow.

Growth was also encouraged by the training of postgraduate students. Although the PDI ceased functioning as an entity in October 2007 due to changes in funding and research direction, it received two major amounts of government funding for projects, Science Vote funding from Mintek and funding from the DST/NRF Centre of Excellence in Strong Materials.

Collaborations were started Fachhochschule Jena and Bayreuth University in Germany, and with Leeds, Cambridge, and Oxford Universities in the UK. In South Africa, the Universities of the Witwatersrand, Cape Town, Limpopo, Nelson Mandela Metropolitan University, the Western Cape and Free State and the CSIR have also been included. Although the work is still ongoing, to date there have been 18 postgraduate students involved (11 have graduated; in total 6 PhDs and 12 MScs), and over 80 journal and conference papers have been published. Various other groups around the world are also working on high temperature replacements for NBSAs and the review[28] also compared the properties of the Pt-based alloys with those of their competitors.

The advantages of the Pt-based alloys are their good strength and oxidation resistance, but their main disadvantages are price and density. Ceramics have good strength and excellent oxidation resistance, but are prone to brittleness. Various Nb-silicides demonstrate good mechanical properties at high temperatures and oxidation resistance, but not at the same compositions[29].

The first part of the work was the selection of the base alloy system, Pt-Al-Cr-Ru, and this was achieved by studying the effect of ternary additions on selected potential binary alloys[30]. Published phase diagram information was used to choose two-phase alloys that could have suitable structures, and the alloys were manufactured by arc-melting elemental constituents of at least 99.9% purity in an argon atmosphere. The alloys were evaluated for a two-phase microstructure, good mechanical properties and oxidation resistance[31]. The microstructure was ascertained by characterization in an SEM, using EDS, and the properties were assessed by simple hardness tests and checking for ductility by studying the cracks. The best samples were then subjected to room temperature and high temperature compression tests, and the results were compared. The results of the high temperature tests are shown in Figure 1, and it can be seen that the proof stress decreases with increasing temperature, and there was a large decrease between 800°C and 1100°C. The best samples were those with Ta and Ti additions.

As part of the characterization, the precipitate distribution after a small amount of deformation was observed using samples prepared for transmission electron microscopy (TEM)[32]. All the precipitates showed a definite bimodal distribution, and perhaps even a trimodal distribution. It was found that Ti, Cr and Ta partitioned to ~Pt_3Al, and stabilized the cubic $L1_2$ structure, giving precipitates of cuboid appearance. The Ru and Ir additions partitioned to the matrix, and the precipitates transformed to the D0′c structure, and had a more complex shape, and were often 'ogdoadically-diced'[33]. The two morphologies are given in Figure 2.

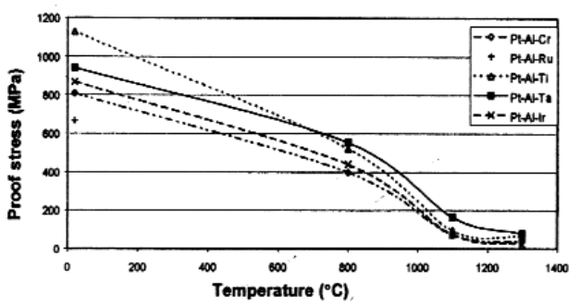

Figure 1—Effect of temperature on the 0.2% proof stress of Pt-Al-X alloys tested at a strain rate of $10^{-4}.s^{-1}$

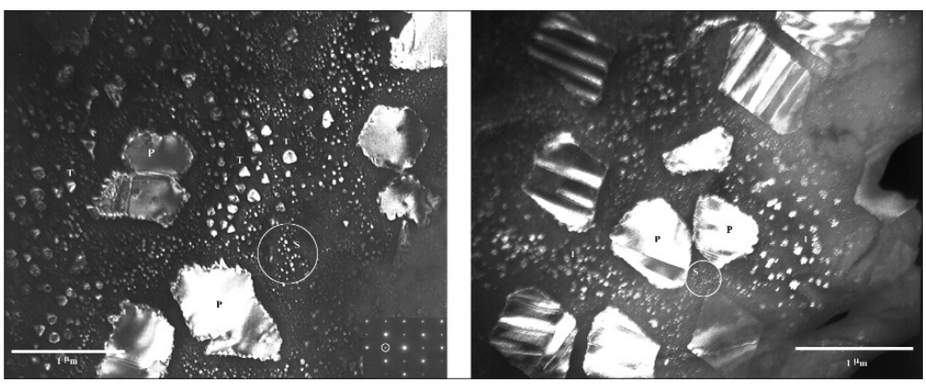

Figure 2—(a) Typical TEM micrograph of the L12 Pt3Al precipitates stabilized by Cr, Ta and Ti addition. P, T and S indicates the different size ranges of the precipitates. Inset shows the selected areas diffraction (SAD) pattern, confirming the L12 structure. (b) Typical TEM micrograph of the D0′c precipitates stabilised by Ru and Ir additions. P, I and S indicate the different size ranges of the precipitates

Overview of the development of new Pt-based alloys

Table I

Comparative lattice misfits of selected $Pt_{86}:Al_{10}:X_4$ alloys

Alloy	Room temperature			
	$a_{(Pt)}$ (nm)	a_{Pt3Al} (nm)	Mismatch[35]	δ[36]
$Pt_{86}:Al_{10}:Ti_4$	3.8921	3.8642	-0.72	-0.0072
$Pt_{86}:Al_{10}:Cr_4$	3.9022	3.8741	-0.72	-0.0072
$Pt_{86}:Al_{10}:Ru_4$	3.9001	3.8530	-1.2	-0.0121
$Pt_{86}:Al_{10}:Ta_4$	3.8941	3.8682	-0.67	-0.0067
$Pt_{86}:Al_{10}:Ir_4$	3.8983	3.8507	-1.2	-0.0123
	800°C			
	$a_{(Pt)}$ (nm)	a_{Pt3Al} (nm)	Mismatch[35]	δ[36]
$Pt_{86}:Al_{10}:Ti_4$	3.9246	3.8961	-0.72	-0.0073
$Pt_{86}:Al_{10}:Cr_4$	3.9390	3.9103	-0.72	-0.0073
$Pt_{86}:Al_{10}:Ru_4$	3.9349	3.8967	-0.97	-0.0098
$Pt_{86}:Al_{10}:Ta_4$	3.9246	3.8961	-0.72	-0.0073
$Pt_{86}:Al_{10}:Ta_4$	3.9246	3.8747	-1.2	-0.0128

Additionally, the displacive transformation producing the D0′c tetragonal structure[22,23] gave distinct bands in the precipitates, and these could be seen to be twin boundaries at higher magnifications[34].

The misfits between the matrix and precipitate phases were also measured[32] at room and high temperature (800°) by X-ray diffraction (XRD). XRD was conducted on a JEOL JDX 3500 diffractometer, operating at 35 kV and 200 mA, with a copper source. The (220) peak was used to derive the (Pt) lattice parameters, (112) was used for tetragonal D0′c Pt_3Al, and (211) was used for cubic L12 Pt_3Al. It must be remembered that the samples either had the cubic of the tetragonal form of Pt_3Al, not both. These measurements were then used to derive the misfits, firstly using a method used for precipitates generally[35]:

$$\text{Lattice misfit} = (a_{ppt} - a_{matrix}) / a_{matrix} \times 100 \quad [1]$$

and secondly, using the more usual expression which is more commonly applied for nickel-based superalloys[36] (but is actually equivalent):

$$\text{Misfit, } \delta = 2 \times ((appt - amatrix) / (appt + amatrix)) \quad [2]$$

with the results given in Table I. The misfits were all negative, and the smaller misfits were associated with the cuboid precipitates of cubic L12 Pt_3Al, whereas the larger misfits correlated with the transformed structure, D0′c Pt_3Al.

The oxidation tests were done by studying the mass difference after a range of isothermal tests at 1350°C under static air. Samples were removed from the furnace at intervals of 1, 10, 25, 100, 500 and 1 000 hours. There was no physical evidence of spalled scale, and the oxide morphologies of the flat samples were examined after testing using scanning electron microscopy (SEM), then mounted edge-on in order to compare the thicknesses of the oxide scale. From the initial study, alloys with aluminium additions exhibited the best oxidation resistance and further Pt-Al-X (where X is another metal) alloys were made and tested more rigorously[20,31–37]. A critical threshold of at least 9 at.% aluminium was found to be necessary for the formation of a stable oxide layer[38,39]. The best creep compression test properties were found for Pt-Al-Ta, Pt-Al-Cr and Pt-Al-Ru[40]. However, the oxidation resistance of the Ta- and Ti-containing alloys was inferior, and thus no further work on Pt-Al-Ta alloys was done[38].

A four-component alloy was selected on the basis that Cr additions gave good mechanical properties, and Ru was seen as a way to increase the volume fraction of the precipitates, as well as improving the strength of the matrix phase[32]. After work on a number of samples, the composition was optimized as $Pt_{84}:Al_{11}:Cr_3:Ru_2$, which gave the best microstructure, as shown in Figure 3.

Ongoing research work at Mintek

Much work has been done since the last review[30], and the future work will be more concerned with commercialization[41]. The underlying research is still very important and will still continue, but other factors, which are more important to commercialization, are also being studied. Although the main alloy is $Pt_{84}:Al_{11}:Cr_3:Ru_2$, the effect of other additions on mechanical properties has also been studied. Cobalt was found to be beneficial for formability[42], while Pd and Ni were substituted for platinum in an attempt to reduce the density and costs. However, the Ni and Pd additions were disappointing in that there was no beneficial effect—indeed, the strength decreased. Work done at the University of Bayreuth and the Fachhochschule Jena in Germany had more favourable results with Ni, but did not use Ru[16]. To complement the study of the extra alloying elements, phase diagram work was also undertaken on the Pt-Ni-Ru[43], Pt-Co-Ru, Pt-Co-Cr and Pt-Cr-Ni[44] systems. More work has also been done on the Pt-Cr-Ru[45,46] and Pt-Al-Co[42] systems.

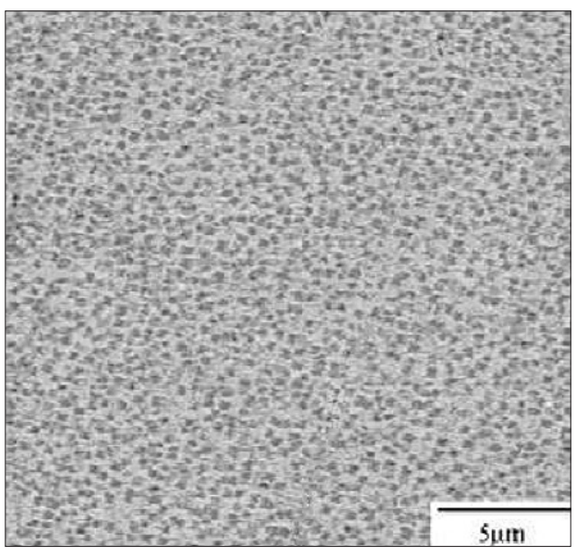

Figure 3—SEM image in backscattered electron of $Pt_{84}:Al_{11}:Cr_3:Ru_2$ showing ~Pt_3Al precipitates (dark) in a Pt-based matrix (light)

Transmission electron microscopy

Introduction

Although Pt-Al was identified as the basis for the alloys[30], ternary additions were made to stabilize the high temperature $L1_2$ cubic form of ~Pt_3Al. Without these additions, a martensitic transformation occurred in ~Pt_3Al forming $D0_c'$ twin-like bands[30,47]. Since the interaction of dislocations in the matrix with the strain field of coherent or semi-coherent precipitates determines the mechanical properties, a rigorous TEM study was made on a series of Pt_{86}:Al_{10}:X_4 alloys where X = Cr, Ru, Ti, Ir and Ta (at.%) to analyse the dislocation content, precipitation and microstructure of samples compressed to a true strain of about 3% at different temperatures (21, 800, 1000 and 1300°C)[48]. Lattice parameters of the (Pt) matrix phase in Pt-Al-X (X = Ru, Cr and Ti) alloys were determined by using selected area electron diffraction (SAED). All patterns were of the <112>-zone type. The results differed slightly from those reported by Hill *et al.*[32], which could be attributed to miscalibration of the microscope's camera[48]. In addition, an unusual ordering phenomenon was found in the Pt_3Al precipitates in the binary Pt-Al alloy[34].

Pt-Al-Cr

There are indications that the precipitates were not cuboidal, but octahedral in nature. The density of small precipitates decreased with increasing compression temperature, while the dislocation density in the matrix increased. The structure of the dislocation system remained the same—no other slip systems were activated at higher temperatures.

Pt-Al-Ru

The morphology of these precipitates differed markedly from those of the Pt-Al-Cr sample. They were 'ogdoadically-diced'[33] (otherwise described as cruciform or Maltese Cross-shaped) similar to those shown in Figure 3, generally consisting of eight interconnected lobes (four in cross-section). The precipitates showed twinned regions, showing that a martensitic transformation to the lower temperature $D0_c'$ form of ~Pt_3Al had occurred, and the Ru addition could not stabilize the cubic $L1_2$ form ~Pt_3Al. Their edges were curved, showing high surface energy for their boundaries, but became more regular at higher compression temperatures. The twin bands also became better developed at higher temperatures, with dislocations found in alternating twin bands. Dislocations occurred in pairs, indicative of superlattice dislocations, which are expected in the ordered structure of these precipitates (just as in the γ' phase of NBSAs).

Pt-Al-Ti

Compressed at 20°C, the precipitates had well-defined, straight borders. They contained no dislocations, although the matrix had a high density of dislocation tangles. With compression at 800°C, there were still no dislocations present within the precipitates, while the dislocation density in the matrix was significantly lower. There was also a high density of smaller precipitates in the matrix, which could add to strengthening of the matrix. Only when compression was done at 1100°C, were dislocations observed in the precipitates. They shared the same Burger's vector as the dislocations in the other alloys: ±1/2<110>. The low density of dislocations in the matrix indicates significant recovery at elevated temperatures. At 1300°C, the precipitates were once again devoid of dislocations, possibly due to recovery at this elevated temperature.

Pt-Al-Ir

The precipitates appeared similar to those in the Pt-Al-Ru sample. No dislocations were seen in the precipitates themselves, although some dislocations in the matrix extended to the precipitate/matrix interface. There were three different precipitate sizes, with the smallest surrounding the largest precipitates, but separated by a depleted zone. SAED revealed that there was only one type of precipitate, although they were found in three different size ranges. The precipitate structure reveals that the small particles surrounding the largest particles were dissolving to aid the coarsening, which would not be a satisfactory high temperature structure. After compression at 800°C, the precipitate edges straightened (although their corners were still round) and the first dislocations appeared in the precipitate. Isolated dislocations traversed the matrix. At 1100°C, most of the 'ogdoadically-diced' (cruciform shaped) precipitates had become spherical. Twin bands were still visible, with dislocation pairs in some. Multiple twinning occurred in the precipitates. At 1300°C, the precipitates were more irregular. The dislocation density was high, and they threaded through all twin bands, not only alternating bands, implying that a second slip system became operative at the higher temperature.

Pt-Al-Ta

The precipitates had straight interfaces with a high density of interfacial dislocations, and a low density within the precipitates. Isolated tangles of mixed screw and edge dislocations were observed in the matrix. At 800°C in compression, irregular precipitates were observed with no dislocations, while the matrix had a high density of dislocations and small cubic precipitates were also evident. At 1100°C, the matrix dislocations disappeared, while the precipitates (which were now more regular) contained dislocations. At 1300°C, the interfaces of the precipitates were much better defined. However, the character of the dislocations inside the precipitates seemed to have changed. From a dislocation viewpoint, this alloy was the strongest, but earlier work[30,37] had shown that the oxidation resistance was insufficient.

High temperature TEM work

Recently, work that could not be done in South Africa was undertaken at the National Institution of Materials Science (NIMS), Japan. One aim was to investigate the changes in the microstructure of a binary Pt-Al alloy and a ternary Pt-Al-Ir alloy at elevated temperatures using *in situ* heating up to 1100°C in a JEOL 4000X TEM. The heating rate used was 10°C/min, with 5°C being used when more detailed changes were to be observed. It is important to be able to study the

stability of the different Pt_3Al phases because the higher temperature cubic form is preferred and is more ductile. Different alloying additions are known to stabilize the high temperature form: Cr, Ti, Ta[32] and Zr, Hf, Mn, Fe and Co[15]. The alloy studied was a binary Pt-Al alloy with the approximate composition Pt_{85}:Al_{15} that is within the two-phase region consisting of the Pt solid solution phase (Pt) and the Pt_3Al phase (γ'). There are two conflicting phase diagrams of the transformation temperatures of γ' Pt_3Al. According to McAlister and Kahan[22], there is a transformation of the high temperature Pt_3Al phase from $L1_2$ to a tetragonal low temperature variant (designated D0'c) at ~1280°C. However, Oya *et al.*[23] showed an additional transformation at a lower temperature. The transformation temperatures given by Oya *et al.*[23] are $\gamma' \rightarrow \gamma'_1$ at ~340°C and $\gamma'1 \rightarrow \gamma'_2$ at 127°C. Previous attempts to resolve this conundrum by SEM, XRD and DTA had been unsuccessful, which prompted the investigation of these transformation temperatures using *in situ* heating of the alloy in a TEM.

Figure 4 shows the microstructure of the binary Pt-Al alloy before heating. Pt_3Al with the lower temperature structure, $D0_c'$, contains well-defined martensite-like twin bands[30].

The precipitate shown in Figure 5 is orientated such that the twin contrast is not visible—this is due to the limitations of the *in situ* heating sample holder, which has only a single axis of rotation. The precipitate in Figure 5 contains two alternating types of bands: one with no dislocations (black arrow) and one that contains a high density of dislocations (white arrow), which corresponds with the spacing of the twin bands[20]. The number of dislocations decreased with increasing temperature (and time), which indicates that there is a transformation that takes place. Although the decrease in dislocation density could be due to a relaxation of the interface misfit due to thermal expansion, it was unlikely in this case because the alternating band nature of the precipitates disappeared at higher temperatures, thus showing that a displacive phase transformation and, hence, a crystal structure transformation, had taken place. The observed changes in contrast occurred at temperatures close to those suggested by Oya *et al.*[23], suggesting that a transformation had taken place, but it does not say anything about the kinetics or transformation temperatures. The transformation was also observed in diffraction mode where the diffraction patterns of the phases were different, and this confirmed that the phase diagram of Oya *et al.*[23] for the Pt-Al system is more accurate than that of McAlister and Kahan[22].

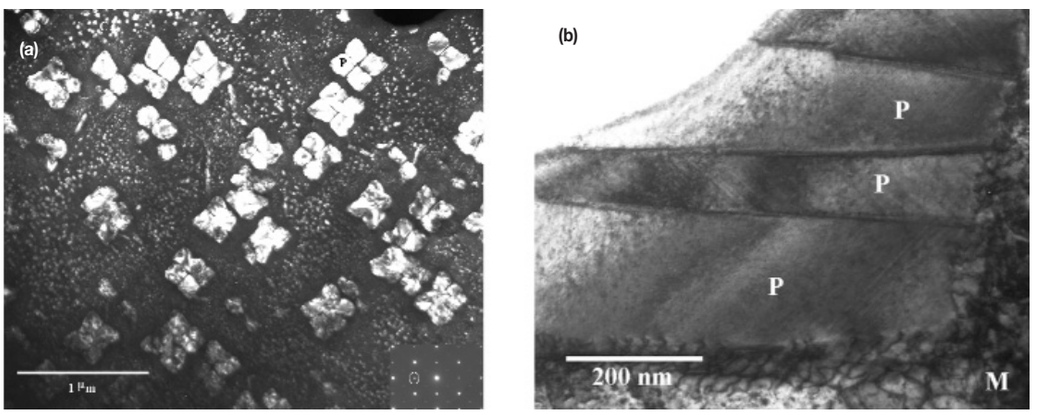

Figure 4—(a) Dark field TEM micrograph of the microstructure of a typical room temperature compressed Pt_{86}:Al_{10}:Ir_4 alloy, with P denoting an ogdoadically-diced precipitates (insert: SAED pattern with reflection used to obtain image circled). (b) Bright field TEM image of a Pt_3Al precipitate showing well-defined twin bands (P)

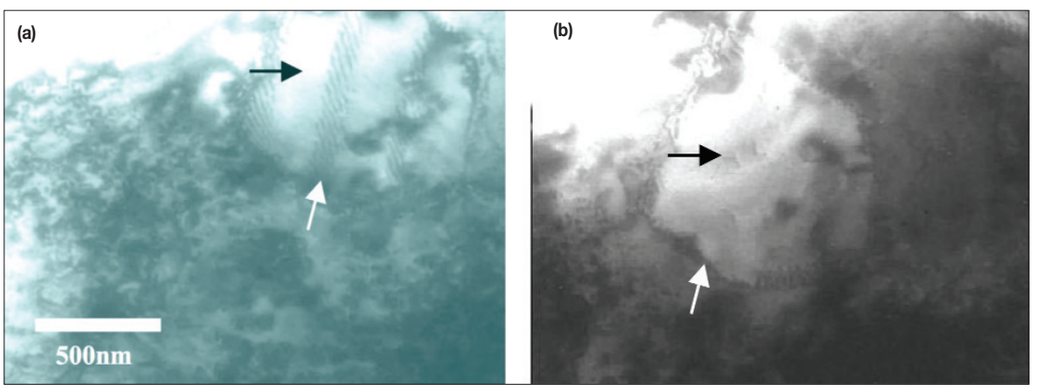

Figure 5—Bright field TEM images of a Pt_3Al precipitate with increasing temperatures. (a) 54°C (b) 477°C

Overview of the development of new Pt-based alloys

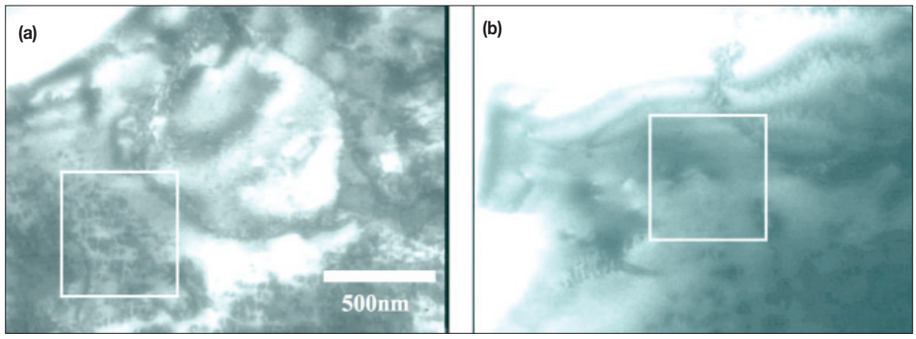

Figure 6—Bright field TEM micrographs showing the dissolution of small precipitates at increasing temperatures, (a) 580°C (b) 870°C

The strength of the alloy depends in part on the presence of small precipitates to act as a barrier to dislocation motion. Ideally, the precipitates should persist at high temperatures to provide strengthening under extreme temperature conditions, but this does not happen in the Pt-Al binary system under consideration. The experimental evidence is shown in Figure 3. The same precipitate is shown in the bright field TEM images, Figure 6 (a)–(b).There is a high density of small precipitates (with the exception of a precipitate-free zone around the large precipitate) in the matrix surrounding the large precipitate at 580°C, as shown in Figure 6 (a). At 810°C, the small precipitates start to dissolve in the matrix. Between 810°C and 870°C precipitate dissolution occurs rapidly, since most of the small precipitates have disappeared at 870°C, as seen in Figure 3(b). All the small precipitates have disappeared at 960°C, implying reduced precipitate strengthening at high temperatures, although the contributions of the different sized precipitates have not yet been ascertained. The large precipitate was noticeably smaller at 1170°C than at 1030°C, and the interfacial dislocation network had completely disappeared.

Results of tensile tests

No tensile tests had been done on any of these Pt alloys before, and interested manufacturers represented at international conferences have asked for tensile data (especially yield and ultimate tensile stress). The first tests were done at Mintek. Since results become strain rate dependent very soon at high temperatures, it was decided to evaluate only the room temperature tensile properties of the best ternary alloys, compared with that of the quaternary alloy. Creep testing of the quaternary alloy will be done at high temperatures at a later stage. It has been shown that the high temperature compressive strength of Pt_{84}:Al_{11}:Ru_2:Cr_3 is significantly higher than that of Pt_{86}:Al_{10}:Cr_4[49,50].

Macro-scale tensile testing was excluded because of the high material cost. Smaller specimens than the sub-size specimen described by the ASTM standard for tension testing[51], were used. Small specimen test technology has been an integral part of fusion materials development because of limited availability of effective irradiation volumes in test reactors, and has resulted in specimens that are miniaturized versions of their full-scale counterparts[52]. From the required dimensional ratios of ASTM standard[51] and the and published studies of specimen size effects[52–55], it was decided that test specimens 46 mm in total length, 3 mm thick, with gauge width and length 3 mm and 18 mm respectively, would ensure that the tensile values would be comparable to those obtained form a standard specimen. Table II gives the nominal compositions of the experimental samples in atomic and weight percent.

Table II

Nominal compositions of experimental alloys (wt%)

Alloy	at.% or wt%	Pt	Al	Cr	Ru
1	wt%	98.5	1.3	0.2	-
	at.%	86	10	4	-
2	wt%	96.2	1.5	-	2.3
	at.%	86	10	-	4
3	wt%	96.2	1.7	0.9	1.2
	at.%	84	11	3	2

Each 50 g ingot was aged in air in a muffle furnace at 1250°C for 100 hours and quenched in water to achieve a homogeneous two-phase microstructure without primary ~Pt_3Al. Flat mini-tensile specimens were machined from each ingot by wire spark erosion. Tensile tests were performed with a cross-head speed of 5 mm/min. Due to the specific set-up of the test and imperfections of some of the specimens' shoulders, calibration of the extensometer was problematic and was set up on a gauge length of 12.5 mm only. Unfortunately, this resulted in inaccurate strain results and elongation was estimated by measuring the distance between gauge marks before and after testing (fractured surfaces of the specimen fitted together), while yield stress could not be determined either.

After testing, one half of each sample was prepared for metallography and Vickers hardness tests (20 kg weight) were performed, followed by SEM analysis in backscattered electron (BSE) mode, as well as energy dispersive X-ray spectrometry (EDX). In general, there were no significant discrepancies between the nominal and actual compositions. Alloy 1 was contaminated by an insignificant amount of Ru (equating to a meagre ~0.01 wt%), while Alloy 2 was contaminated by ~0.05 wt% Cr. The contamination was probably the result of some minor sputtering in the button-

arc furnace during melting. Subsequently, TEM specimens were also manufactured, and examined in a Philips CM200 TEM. X-ray diffraction (XRD) analyses were conducted on the polished samples using Mo Kα radiation. All samples except for the Ru alloy, which was single-phase (Pt) (i.e. Pt-based solid solution), comprised both (Pt) and ~Pt_3Al. The fracture surfaces of the other half of each sample were also examined using SEM in secondary electron (SE) mode.

It has been shown before that Ru is, in fact, a better solid solution strengthener in these alloys than Cr[32], and therefore the fact that the Pt_{86}:Al_{10}:Cr_4 specimens were stronger than those of Pt_{86}:Al_{10}:Ru_4 could be explained only by a low volume fraction (~5%) of ~Pt_3Al precipitates that was present in the Ru alloy. This was confirmed by both XRD and TEM[56], and implied that Pt_{86}:Al_{10}:Ru_4 had been annealed above its solvus, which was thought to be between 1250°C and 1300°C[57]. Thus, the higher ductility of this alloy was due to its nearly single phase (Pt) nature.

The presence of ~Pt_3Al in the Pt_{84}:Al_{11}:Ru_2:Cr_3 specimens was confirmed by XRD and TEM. The volume fraction of precipitates varied from specimen to specimen. Some of the specimens failed outside the gauge length, and discarding these, the average hardnesses, maximum UTS and estimated elongation for each alloy are given in Table III.

Pt_{86}:Al_{10}:Cr_4 was harder and also had a higher UTS than Pt_{86}:Al_{10}:Ru_4. However, Pt_{84}:Al_{11}:Ru_2:Cr_3, with a significant volume fraction of ~Pt_3Al, was the hardest, but had the lowest UTS of the three alloys. This was also the only alloy that failed intergranularly, while the others failed mainly by intragranular cleavage with some localized signs of dimpling. It is likely that the lower UTS was related to the intergranular failure mode, which correlates to its lower elongation.

The spread and inconsistencies in the results were disappointing. It would have been more ideal to test a wider range of specimens, but working with Pt always constrains the experimental matrix because of the expense.

One can, however, conclude that these Pt-based alloys are in the order of 300–350 HV with a UTS of ~800MPa[56,58]. To compare with other alloys, this is significantly higher than the 40–50 HV of pure Pt in the soft state and its UTS of ~140 MPa[59]. Compared to other high-temperature alloys, such as the ferritic ODS alloy PM2000, which has a room temperature UTS of 720 MPa and elongation of 14% at room temperature[60], γ-TiAl with UTS of 950 MPa and elongation of ~1%[61] and CMSX-4 with UTS 870 MPa[62] it is obvious that these Pt-based alloys are within range of these type of alloys, which is encouraging considering the as-yet unoptimized nature of their heat treatments and microstructures.

Commercialization plans

The ultimate target for the Pt-based alloys is the land-based turbine industry. However, as this is such a difficult market to penetrate, penetration might be accomplished only once turbine engines have been radically designed to exploit the ~200°C increase in application temperature. Thus, in the interim, it has been decided to initially target other applications, thereby providing recognition for these alloys as useful industrial materials. The ultimate aim has not changed, and is still being actively pursued, but using the alloys in other applications could help speed up their acceptance in the turbine industry, while simultaneously increasing the overall use of platinum. Several niches have been identified, all of which require good strength at high temperatures in aggressive environments. Three main directions are being targeted for potential commercialization: casting, coatings and powder metallurgy. Casting was selected because most components are initially cast before any other forming operation, and it is important to demonstrate the alloys' castability. The other two niches are for different forming mechanisms.

Powder metallurgy

Another potential niche is powder metallurgy, which gives good properties with minimal waste. This technique is used when the component is difficult (or impossible) to fabricate by cheaper methods, and excellent properties are needed. It can also be used to shape mixtures of powders. Since the targeted application is for high temperature in aggressive environments, it is likely that some of the components currently being targeted, such as valves and nozzles, might need to be made via powder methods. Many of these types of components are already being manufactured by powder methods in order to get the good properties required or because of their intricate shapes.

Coatings

A second niche is using the alloys as coatings on a cheaper substrate, such as a stainless steel. Coatings are employed for a variety of reasons including attractiveness, corrosion resistance and/or wear resistance. Coatings can be preferable for cheaper components, or where the component is not needed to last so long. Thus, it is more economical to coat a cheaper substrate with a more expensive alloy than to have the whole component being made from the expensive alloy. Coatings can also be advantageous where low weight is important. The Pt-based alloys are dense, so using these alloys as coatings would provide their benefits combined with the reduced density of a lighter substrate. This part of the project compliments powder metallurgy because the powders can be a source for the coatings. Although coatings on NBSAs are being targeted initially, other niches include chemical plants, marine environments, and the automotive industry.

Table III

Room temperature mechanical properties of experimental alloys

Alloy	Alloy composition (at.%)	Hardness (HV10)	Maximum ultimate tensile strength achieved (MPa)	Elongation (%)
1	Pt_{86}:Al_{10}:Cr_4	317 ± 13	836	~4
2	Pt_{86}:Al_{10}:Ru_4	278 ± 14	814	~9
3	Pt_{84}:Al_{11}:Ru_2:Cr_3	361 ± 10	722	~1

Overview of the development of new Pt-based alloys

Ongoing research work at Fachhochschule Jena and the University of Bayreuth, Germany

The starting point for the development programme for precipitation hardened Pt alloys at the University Bayreuth and the Fachhochschule Jena-University of Applied Sciences were the ternary Pt-Al-X, alloys which had already been investigated by the South African group at Mintek[40]. These results[40] were very promising, especially for the $Pt_{86}:Al_{10}:Cr_4$ alloy, which having relatively high stress-rupture strength as well as good ductility (Figure 7) was selected for further optimization[63].

Quaternary Pt-Al-Cr-Ni alloys

Since nickel has a good solid-solution strengthening effect on the (Pt) matrix[64], it was added to a Pt-Al-Cr alloy in varying amounts[15]. Nominal compositions of the alloys preserved a Pt:Al:Cr ratio of about 86:11:3, in keeping with preceding results on the alloy $Pt_{86}:Al_{10}:Cr_4$[40]. $Pt_{86\text{-}76}:Al_{11}:Cr_3:Ni_{0\text{–}10}$ alloys with up to 10 at.% Ni were melted.

Alloying the Pt-Al system with both Cr and Ni consistently stabilized the $L1_2$ high temperature modification of Pt_3Al at room temperature. $Pt_{86\text{-}76}:Al_{11}:Cr_3:Ni_{0\text{–}10}$ alloys were all single phase after solution heat treatment at 1450°C. Ageing at 1000°C produced microstructures similar to Ni-based superalloys. Precipitates in alloys with less than 6 at.% Ni appear to lose coherency after ageing[15]. The alloy $Pt_{80}:Al_{11}:Cr_3:Ni_6$ after ageing not only had the highest γ' volume fraction, ~23%, but also had well-aligned cuboid precipitates with 0.2–0.5 μm edge lengths and a misfit of -0.1%, similar to Ni-base superalloys. Spherical particles were observed in alloys with more than 6 at.% Ni. These changes of γ' morphologies were correlated to a decreasing values of the misfits with increasing Ni concentration, so that positive values gave round ~Pt_3Al precipitates, values of ~–0.0001 gave a cuboid morphology, and values of ~–0.005 gave an irregular morphology[65]. Ageing at 1100°C lead to coarse γ' particles and reduced γ' volume fractions. However, volume fractions decreased less with temperature in alloys containing Ni than in those without Ni.

Variation of the Al content for high γ' volume fraction

$Pt\text{-}Al_{12\text{–}15}:Cr_3:Ni_{4\text{–}8}$ alloys with Al contents from 12–15 at.% were chosen near the solubility limit of about 15 at.% in order to achieve high γ' volume fractions[15-16]. Alloys with up to 13 at.% Al were successfully homogenized in the single phase γ-region at 1500°C, and still higher Al contents led to eutectic two-phase interdendritics even after heat treating at 1530°C.

Ageing alloys with up to 13 at.% Al for 120 h at 1000°C led to homogeneous distributions of Pt_3Al particles. Alloy $Pt\text{-}Al_{14}:Cr_3:Ni_6$ showed cubic Pt_3Al particles with 520 μm average edge lengths (Figure 8b), hence a microstructure very close to that of Ni-based superalloys. The absolute lattice misfit between γ and γ' decreased with increasing Ni content. Once again, slightly negative misfit values measured at room temperature together with cubic or spherical particles[65], respectively, signified coherency between γ and γ' in alloys with more than 5 at.% Ni (Figure 8b and c). A lack of coherency was apparent in the alloy with Ni content below 5 at.% and high negative misfit of about -0.5 % (Figure 8a). By raising the concentration of the major γ'-forming element Al up to 13 at.% the γ' volume fraction could be increased to 30%[16].

Variation of the Cr γ' volume fraction

The Al content in Pt-Al-Cr-Ni alloys is limited to about 12.5 at.%[13]. In another test series, the composition range was $Pt\text{-}Al_{12.5}:Cr_{0\text{–}6}:Ni_6$ in order to ensure coherency between γ and

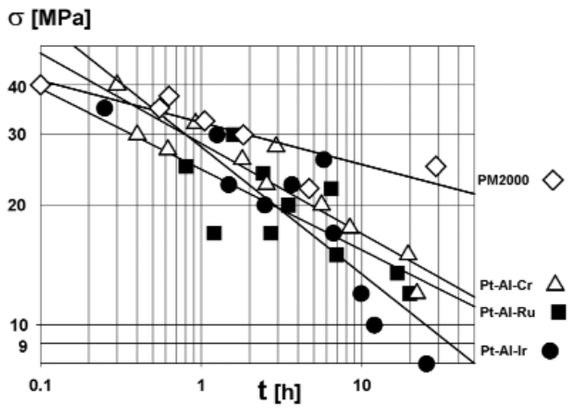

Figure 7—Stress-rupture curves of PM2000 and $Pt_{86}:Al_{10}:Z_4$ alloys at 1300°C (Z = Cr, Ru or Ir)[40]

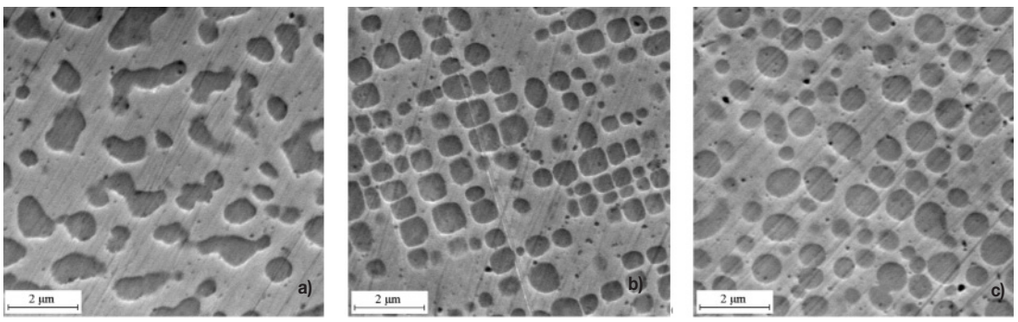

Figure 8—Secondary electron SEM micrographs of the investigated alloys, annealed for 12 h at 1500°C and 120 h at 1000°C in Ar. The dark areas are precipitates, the brighter areas the matrix phase. (a) $Pt\text{-}Al_{14}:Cr_3:Ni_4$, (b) $Pt\text{-}Al_{14}:Cr_3:Ni_6$, (c) $Pt\text{-}Al_{14}:Cr_3:Ni_8$

Overview of the development of new Pt-based alloys

γ'. Dendritic as-cast structures of Pt-$Al_{12.5}$:Cr_3:Ni_6, Pt-Al_{12}:Ni_6 and Pt-Al_{12}:Cr_6:Ni_6 could be homogenized by heat treatment at 1500–1510°C[14–16]. Formation of Pt_3Al precipitates was almost completely suppressed in Pt-$Al_{12.5}$:Cr_3:Ni_6 after homogenization for 12 h at 1500°C and subsequent water quenching (Figure 9a). Air cooling lead to homogeneous distributions of Pt_3Al particles with 200 μm average edge lengths and a volume fraction of about 30% (Figure 9b). Furnace cooling from 1500°C produced a bimodal particle distribution with a coarse particle fraction (Figure 9c), with an entire γ' volume fraction of 34%. Increasing the Cr content to 6 at.% lead to average edge lengths of 500 μm and a volume fraction of 50% in Pt-Al_{12}:Cr_6:Ni_6 after homogenization for 6 h at 1500°C + 6 h at 1510°C in Ar, followed by air cooling. For these Pt-based superalloys, controlled air cooling after solution heat treatment is sufficient to achieve the targeted microstructure similar to Ni-based superalloys.

Substitution of Ni

In a trial and error approach, the high melting elements Nb, Ta and Ti were chosen[14-16] to substitute Ni. By XRD analysis, the fcc γ matrix and the $L1_2$-ordered γ' Pt_3Al phases were identified in Pt-Al_7:Cr_6:Nb_5, Pt-Al_7:Cr_6:Ta_5 and Pt-Al_7:Cr_6:Ti_5. The lattice misfit ratios were ~–3 x 10^{-3} in all alloys. After homogenization, the alloys showed bimodal size distributions of the γ' particles (Figure 10a–c). Besides coarse and irregularly shaped particles with a volume fraction between 10 and 20%, small cuboids of up to 300 μm in size were observed. After subsequent ageing for 264 h at 1200°C with water quenching, measurement of the chemical compositions revealed Nb and Ta to be almost evenly distributed within the γ matrix and γ' phase, whereas Ti was enriched in the γ' phase. The γ' volume fractions after ageing was 34% in Pt-Al_7:Cr_6:Nb_5, 33% in Pt-Al_7:Cr_6:Ta_5 and 35% in Pt-Al_7:Cr_6:Ti_5. Compression strengths of polycrystalline Pt-Al_7:Cr_6:Nb_5, Pt-Al_7:Cr_6:Ta_5 and Pt-Al_7:Cr_6:Ti_5 were higher than that of Pt-Al_{12}:Cr_5[40] (Figure 11). At 800°C Pt-Al_7:Cr_6:Ta_5 was strongest, whereas at higher temperatures Pt-Al_7:Cr_6:Nb_5 showed the highest strength. Above 1200°C, Pt-Al_7:Cr_6:Nb_5 and Pt-Al_7:Cr_6:Ta_5 outperformed the single-crystal Ni-based superalloy CMSX-4. The deformed samples indicated rupture on the outside surface, which was also observed in the case of the Nb- and the Ti-containing Pt-based alloys.

Due to the ongoing dissolution of the hardening γ′-phase at very elevated temperatures, the Pt-based superalloys are designed for applications up to 1300°C. Using the equipment[66] illustrated in Figure 12, the stress-rupture curves at 1300°C were determined for Pt 10%Rh, Pt 10%Rh DPH and Pt-Al_{12}:Cr_6:Ni_5 (Figure 13), and the latter has the highest stress rupture strength. The Norton plot was generated by plotting minimum creep rate against stress (Figure 14), using a double logarithmic plot, so that the data points fall on near straight lines. The slope is equal to the Norton exponent n of the Norton creep law in Equation [3]:

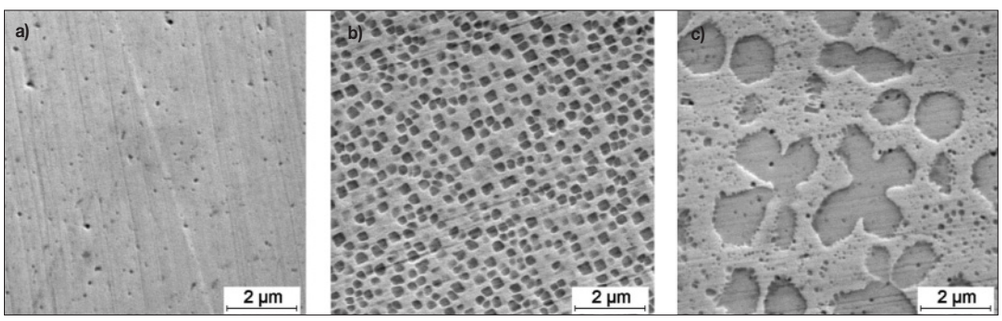

Figure 9—Secondary electron SEM micrographs of Pt-$Al_{12.5}$:Cr_3:Ni_6 after homogenization for 12 h at 1500°C and different cooling regimes. (a) water quenched, (b) air cooled, (c) furnace cooled

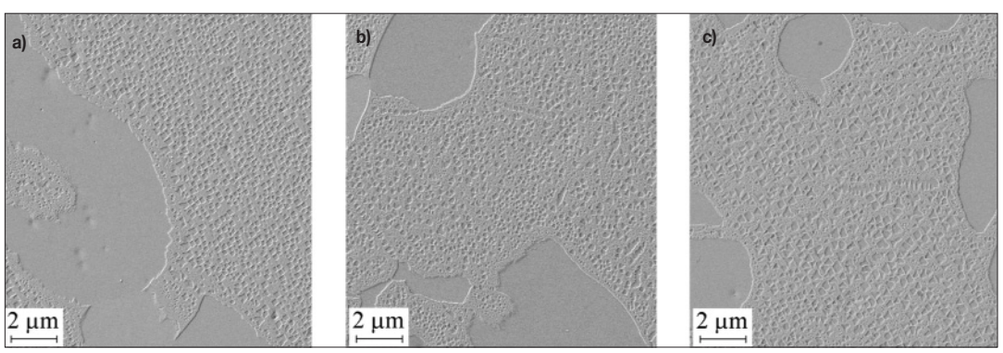

Figure 10—SEM secondary electron micrographs of the γ-γ' microstructures of after heat treatment for 6 h at 1500°C and 6 h at 1510°C with air cooling. (a) Pt-Al_7:Cr_6:Nb_5, (b) Pt-Al_7:Cr_6:Ta_5, (c) Pt-Al_7:Cr_6:Ti_5

Overview of the development of new Pt-based alloys

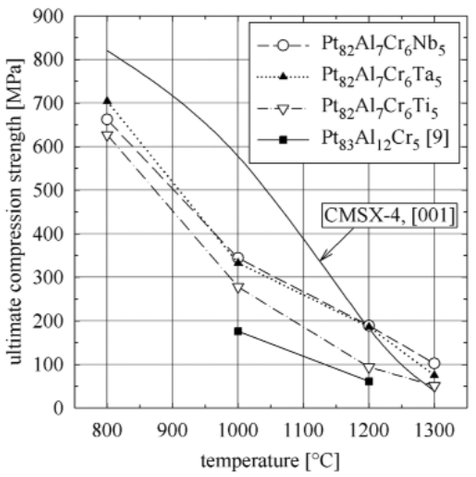

Figure 11—High-temperature compression strength of the polycrystalline Pt-Al-Cr-X alloys[40] and single-crystal Ni-base superalloy CMSX-4

$$\dot{\epsilon}_{min} = A\,\sigma^n \qquad [3]$$

Where A = a constant which is a function of temperature, material, state of the material,

σ = stress in MPa

n = Norton exponent.

The Norton exponent of Pt 10%Rh at a temperature of 1600°C was calculated to be $n = 3.3$, and $A = 34$ (for σ in MPa)[67]. For pure Pt, Völkl *et al.*[6] gave values of $n = 3.8$ and $A = 10^{-5}$ at 1600°C and similar stresses.

The Norton exponent of Pt-Al_{12}:Cr_6:Ni_5 was determined as $n = 3.6$, as shown in Figure 14. The low Norton exponents for pure Pt, Pt 10%Rh and Pt-Al_{12}:Cr_6:Ni_5 are typical for the viscous-drag controlled creep of single-phase solid solution alloys[68,69]. However, the low value of Pt-Al_{12}:Cr_6:Ni_5 could be also explained by the observed intergranular fracture mode in the creep deformed samples, indicating some brittleness and weakness of the grain boundaries. It is expected that once creep tests are undertaken on the specimens with boron (described below), higher Norton exponents and improved creep life are expected.

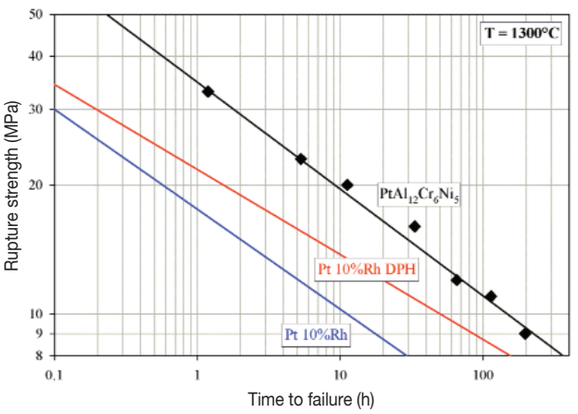

Figure 13—Stress-rupture strength curve of different Pt materials at 1300°C[66]

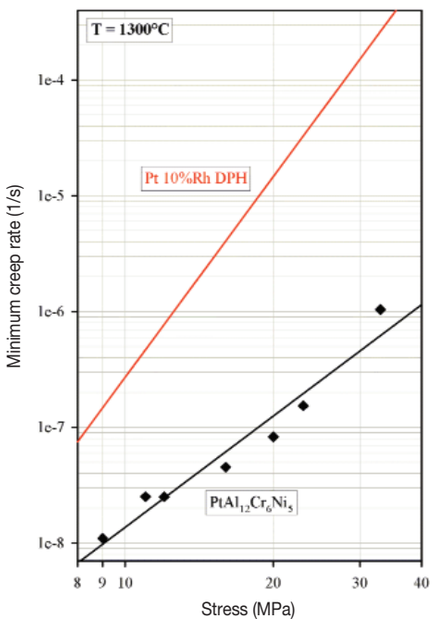

Figure 14—Norton plot of Pt 10%Rh DPH and Pt-Al_{12}:Cr_6:Ni_5 at 1300°C

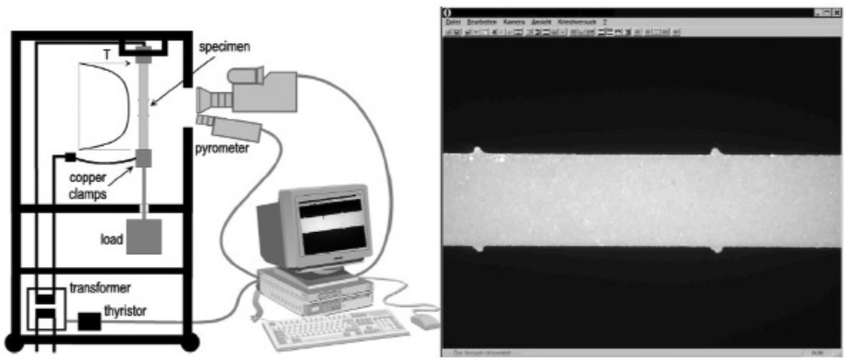

Figure 12—(a) Creep testing facility for tests at constant load either in air or inert gas atmosphere at temperatures up to 3000°C[66]. (b) Screenshot of the software SuperCreep for strain measurements

Overview of the development of new Pt-based alloys

Microalloying

Small boron atoms often segregate to grain boundaries and can therefore influence grain boundary adhesion. Rhenium is very beneficial for the creep strength of Ni-based superalloys. Therefore B and Re were added to Pt-Al_{12}:Cr_6:Ni_5 in various amounts. Compression creep tests at 1200°C revealed that minor B additions increase both creep strength and ductility considerably (Figure 15a). Additions of 0.3 at.% B together with 2 at.% Re further increased creep strength (Figure 15b).

Corrosion studies at the University of the Witwatersrand

Although corrosion testing of platinum-based alloys for the glass industry is well documented[70], corrosion work had not been attempted on the current alloys. The high temperature corrosion behaviour of Mintek's Pt-based superalloys was studied by performing a crucible test[71]. The test was conducted at 950°C to increase the corrosion kinetics. This temperature was selected because it is within the temperature ranges at which hot corrosion is most effective[72-74]. The samples comprised five Pt-based superalloys and two benchmark alloys. The latter were two single-crystal CMSX-4 nickel-based superalloys (NBSAs) of composition Ni-$Cr_{5.7}$:Co_{11}:$Mo_{0.42}$:$W_{5.2}$:$Ta_{5.6}$:$Al_{5.2}$:$Ti_{0.74}$ wt%. A thin platinum aluminide coating [Pt_2Al – $Pt_{67}Al_{33}$ (at.%)] of approximately 1.25 μm thickness was deposited on one of the benchmark alloys, while the other was uncoated. Samples were covered in analytical anhydrous Na_2SO_4 salt, which acted as the corrosive electrolyte inside a 20 ml high alumina crucible that was placed inside a furnace with a static dry air environment. The test was performed for 540 hours, with an initial 60 cycles of 1 hour of heating and 20 minutes of cooling to room temperature, followed by subsequent long cycles of 72 hours of heating. Samples (washed free of salt residues) were weighed at the end of every cycle and fresh salt was provided for every cycle[71].

The corrosion morphology and the cross-sectional analysis of the corroded alloys were characterized by SEM with EDS, XRD, and Raman spectroscopy being used to confirm the phases.

The mass gains of the samples from the crucible test of being immersed in Na_2SO_4 at 900°C for 168 hours are given in Figure 15. After day 3, the tests on the uncoated CMSX-4 specimen were discontinued. It can be seen that there was very little change in mass for the Pt-based alloys, as a result of the formation of the protective scale.

In the case of the uncoated NBSA, initial mass gain was as a result of the formation of oxides, and further reactions and the formation of unprotective oxides resulted in catastrophic corrosion, which led to change in mass[71]. The test was discontinued as the uncoated sample degraded. XRD analysis of the product showed a mixture of compounds based mainly on sodium, and nickel. Conversely, for the Pt-based superalloys, XRD showed that the surface was mainly alumina, which is the oxide coating that forms naturally. This was a good indication that the Pt-based substrate was supporting the alumina layer well. The morphologies of the Pt-based alloys were much better than those of CMSX-4. Pt_{86}:Al_{10}:Cr_4 had the best appearance, and Pt_{84}:Al_{11}:Cr_3: Ru_2 and Pt_{86}:Al_{10}:Ru_4 were slightly pitted, with the latter showing more pits. Pt_{79}:Al_{15}:Co_6 appeared good in places, with losses in other places. However, it must be realized that these pits are small in nature, and negligible when compared with the damage to the NBSA. With the naked eye, no change in appearance could be seen in the Pt-based alloys. The data are shown in Figure 13[71].

Corrosion morphologies were studied in a SEM and both coated and uncoated CSMX-4 samples suffered greater attack than the Pt-based superalloys, forming a nonprotective porous scale[71]. The corroded morphologies of Pt_{73}:Al_{15}:Co_{12} and Pt_{79}:Al_{15}:Co_6 showed a disintegrated scale layer, indicating that the scale was not protective in this environment. The scale morphologies of Pt_{86}:Al_{10}:Cr_4,

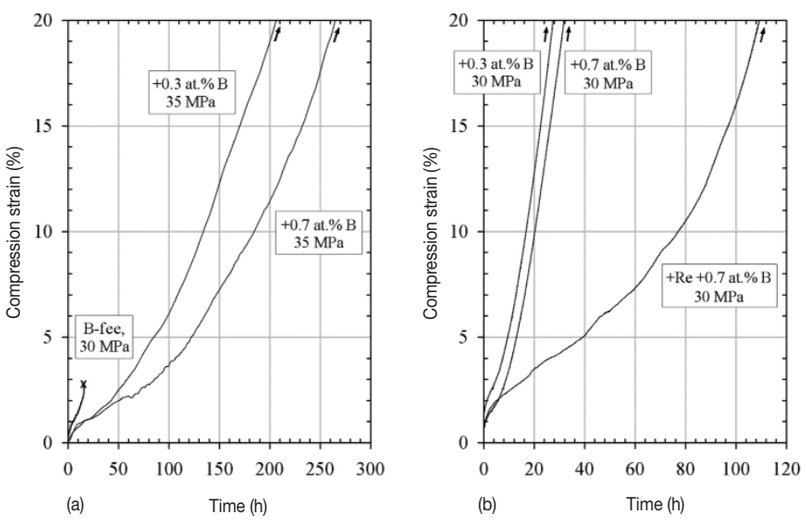

Figure 15—Compression creep curves of pure and micro alloyed Pt-$Al_{12}Cr_6Ni_5$. a) Pure alloy compared to alloys micro alloyed with 0.3 and 0.7 at.% B at 1200°C. b) Alloys micro alloyed with 0.3, 0.7 at.% B and with both 2 at.% Re and 0.7 at.% B at 1300°C

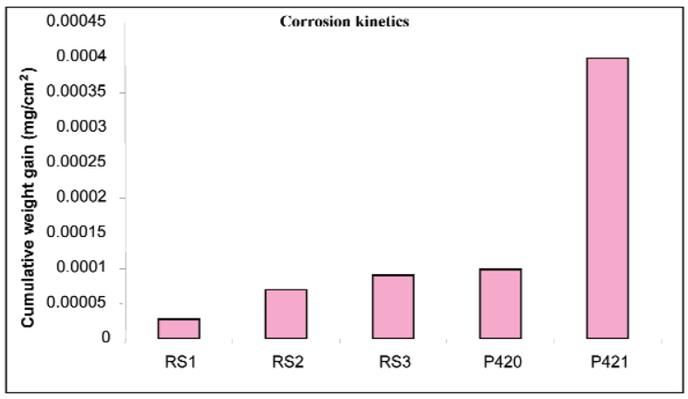

Figure 16—Comparison of mass losses after the crucible test at 950°C. Key: RS1= Pt_{86}:Al_{10}:Cr_4; RS2 = Pt_{86}:Al_{10}:Ru_4; RS3 = Pt_{84}:Al_{11}:Cr_3:Ru_2; P420 = Pt_{79}:Al_{15}:Co_6 and P421 = Pt_{73}:Al_{15}:Co_{12}

Pt_{86}:Al_{10}:Ru_4 and Pt_{84}:Al_{11}:Cr_3:Ru_2 were slightly similar. They were more tenacious and complete, although apparently porous, and gave more protection against hot corrosion than in the Pt-based superalloys with cobalt[71].

SEM micrographs of the cross-sections of samples revealed that there was a very thin oxide film on the surface of alloys Pt_{86}:Al_{10}:Cr_4, Pt_{86}:Al_{10}:Ru_4 and Pt_{84}:Al_{11}:Cr_3:Ru_2, which was not visible using optical microscopy[71]. Although this scale rendered protection against high temperature corrosion, the porous structure did allow some internal attack, observed to depths of ~15μm beneath the scale[71].

Conclusions

At Mintek, the latest research work on the original Pt-based alloys for high temperature applications in aggressive environments has progressed well, and some new alloying additions have been made, for example Ni, Co and Pd. Only the Co additions were beneficial. The first tensile tests of the alloys worldwide have been done at ambient temperature. The results were very encouraging because they were comparable to those of other high temperature alloys. TEM work has shown how the microstructure of the alloys changes at high temperature, and although encouraging, the results suggest that further additions to stabilize the small precipitates would be beneficial above 1300°C, because changes to the microstructure were observed a this temperature.

Work at the Fachhochschule Jean and the University of Bayreuth started from a promising Pt-Al-Cr alloy, and investigated the influence of additions of further elements on mechanical strength and microstructure. Nb, Ta and Ti increased strength when added as partial substitute for Al, although there was higher susceptibility to internal oxidation. After ageing, finely dispersed precipitates in the matrix were observed. Minor additions of B greatly increased creep resistance and rupture time, due to strengthening of the grain boundaries. Rhenium was found to slow down precipitate growth and to increase creep strength further.

Corrosion work at the University of the Witwatersrand demonstrated that the formation of a thin scale on the surface of the three alloys makes the Pt-based superalloys more resistant, although fluxing of this scale decreased protection at high temperatures. The Pt-Al alloys with Cr and/or Ru had the best corrosion resistance, far outperforming both the coated and uncoated CMSX-4 NBSAs; which is very encouraging for the development of Pt-based alloys for applications in gas turbine engines. The Pt-based superalloys with Co performed much better than both NBSAs, but were less stable than alloys with Cr and Ru, owing to the formation of Co oxides, which are more volatile.

Acknowledgements

Bernard Joja is thanked for the SEM work and Chris Fletcher is thanked for undertaking tensile tests. Financial assistance from the South African Department of Science and Technology (DST), the Platinum Development Initiative (PDI: AngloPlat, Impala and Lonmin), NRF/DST Centre of Excellence for Strong Materials, German Science Foundation (DFG) and Japan Society for the Promotion of Science (JSPS) is gratefully acknowledged. This paper is published with permission of Mintek.

References

1. Fischer, B. New Platinum Materials for High Temperature Applications. *Advanced Engineering Materials*, vol. 3, no. 10, 2001. pp. 811–820.

2. Whalen, M.V. Platinum Metals Review, Space Station Resistojets, vol. 32, 1988, no. 1, pp. 2–10.

3. Lupton, D.F. Noble and Refractory Metals for High Temperature Space Applications. *Advanced Materials*, 1990, pp. 29–30.

4. Fischer, B., Freund, D. and Lupton, D.F. Stress-Rupture Strength and Creep Behaviour of Platinum Alloys. *Proceedings 21st International Precious Metals Institute*, San Francisco, USA, 1997, pp. 307–322.

5. Fischer, B., Behrends, A., Freund, D., Lupton, D.F. and Merker, J. Dispersion Hardened Platinum Materials for extreme Conditions. *Proceedings The Minerals, Metals & Materials Society*, San Diego, USA, 1999, pp. 321–331.

6. Völkl, R., Freund, D., Fischer, B. and Gohlke, D. Comparison of the creep and fracture behaviour of non-hardened and oxide dispersion hardened platinum base alloys at temperatures between 1200°C and 1700°C. *Proceedings 8th International Conference on Creep and Fracture of Engineering Materials and Structures*, vol. 171–174, 1999, pp. 77–84.

7. Patent specification 1 340 076, (1973), Johnson Matthey, GB.

8. Patent specification WO 81 / 00977, (1981), Owens-Corning Fiberglass Corporation USA.

9. Patent specification DE 30 30 751 A1, (1982), Degussa AG, Germany.

10. Patent specification DE 31 02 342 C2, (1988), Johnson Matthey, GB.

11. Patent specification DE 44 17 495 C1, (1995), SCHOTT GLAS, Germany.

12. Merker, J., Fischer, B., Völkl, R. and Lupton, D.F. Investigations of New Oxide Dispersion Hardened Platinum Materials in Laboratory Tests and Industrial Applications. *Materials Science Forum*, vol. 426–432, 2003, pp. 1979–1984.

13. Vorberg, S., Wenderoth, M., Glatzel, U., Fischer, B. and Völkl R. Pt-Al-Cr-Ni Superalloys: Heat Treatment and Microstructure, Journal of Minerals. *Metals & Materials Society*, vol. 56, 2004, no. 9, pp. 40–43.

14. Vorberg, S., Wenderoth, M., Glatzel, U., Fischer, B. and Völkl R. A TEM Investigation of the γ/γ' Phase Boundary in Pt-Based Superalloys. *Journal of Minerals, Metals & Materials Society*, vol. 57, 2005, no. 3, pp. 49–51.

15. Hüller, M., Wenderoth, M., Vorberg, S., Fischer, B., Glatzel, U. and Völkl, R. Optimization of Composition and Heat Treatment of Age-Hardened Pt-Al-Cr-Ni Alloys. *Metallurgical and Materials Transactions A*. vol. 36, 2005, pp. 681–689.

16. Wenderoth, M., Cornish, L.A., Süss, R., Vorberg, S., Fischer, B., Glatzel, U. and Völkl, R. On the Development and Investigation of Quaternary Pt-Based Superalloys with Ni Additions. *Metallurgical and Materials Transactions*, A, vol. 36, 2005, pp. 567–575.

17. Völkl, R., Yamabe-Miarai, Y., Huang, C and Harada, H. Stabilizing the $L1_2$ structure of Pt_3Al(r) in the Pt-Al-Sc system. *Metallurgical and Materials Transactions A*, vol. 36, 2005, pp. 2881–2892.

18. Wenderoth, M., Völkl, R., Yokokawa, T., Yamabe-Miarai, Y. and Harada, H. High temperature strength of Pt-base superalloys with different γ' volume fractions. *Scripta Materialia*, vol. 54, 2006, pp. 275–279.

19. Wolff, I.M. and Hill, P.J. Platinum metals-based intermetallics for high temperature service, *Plat. Metals Rev.*, vol. 44, no. 4. 2000. pp. 158–166.

20. Hill, P.J., Adams, N., Biggs, T., Ellis, P., Hohls, T., Taylor, S.S., and Wolff, I.M. Platinum alloys based on Pt–Pt3Al for ultra-high temperature use, *Mat. Sci. Eng. A*, vol. 329-331, 2002. pp. 295–304.

21. Hill, P.J., Biggs, T., Ellis, P., Hohls, T., Taylor, S.S., and Wolff, I.M. An assessment of ternary precipitation-strengthened Pt alloys for ultrahigh temperature applications, *Mater. Sci. Eng. A*, vol. 301A, 2001. pp.167–179.

22. McAlister, A.J. and Kahan, D.J. The Al-Pt (Aluminium-Platinum) System, *Bulletin of Alloy Phase Diagrams*, 1986, vol. 7, pp. 45–51.

23. Oya, Y., Mishima, U., and Suzuki, T. $L1_2 \leftrightarrow D0c$ Martensitic Transformation in Pt_3Al and Pt_3Ga, *Z. Metallkde*, 1987, vol. 78, no. 7, pp. 485–490.

24. Sims, C.T., Stoloff, N.S. and Hagel W.C. *Superalloys II*, Wiley Interscience, USA, 1987.

25. Pope, D.P. and Ezz, S.S., Mechanical properties of Ni_3Al and nickel-base alloys with high volume fraction of γ', *Int. Met. Rev.*, vol. 29, 1984, pp. 136–167.

26. Yamabe-Mitarai, Y., Koizumi, Y., Murakami, Ro, Y., Maruko, T., and Harada, H., Development of Ir-base refractory superalloys, *Scripta Materialia*, 1996, vol. 35, no. 2, pp. 211–215.

27. Yamabe-Mitarai, Y., Koizumi, Y., Murakami, Ro, Y., Maruko, T., and Harada, H., Rh-base refractory superalloys for ultra-high temperature use, *Scripta Materialia*, 1997, vol. 36, no.. 4, pp. 393–398.

28. Cornish, L.A., Fischer, B., and Völkl, Development of platinum-group-metals for high temperature use, Ultrahigh-Temperature Materials for Jet Engines, *MRS Bulletin*, 2004, vol. 28, no. 9, pp. 632–638.

29. Zhao, J.-C., and Westbrook, J.H. Ultra high temperature materials for jet engines, *MRS Bulletin*, 2003, vol. 28, no. 9, pp. 622–627.

30. Cornish, L.A., Süss, R., Chown, L.H., Taylor, S., Glaner, L., Douglas, A. and Prins, S.N. Platinum-based alloys for high temperature and special applications, *International Platinum Conference 'Platinum Adding Value'*, Sun City, South Africa, 3–7 October 2004, South African Institute of Mining and Metallurgy Symposium Series S38, pp. 329–336.

31. Hill, P.J., Cornish, L.A., and Witcomb, M.J. The oxidation behaviour of Pt-Al-X alloys at temperatures between 1473 and 1623 K. *Proc High Temperature Corrosion and Protection 2000*, Sapporo, Japan, 2000. pp. 185–190.

32. Hill, P.J., Yamabe-Miarai, Y., Murakami, H., Cornish, L.A., Witcomb, M.J., Wolff, I.M., and Harada, H. The precipitate morphology and lattice mismatch of ternary (Pt)/Pt_3Al alloys. *Structural Intermetallics 2001*. Hemker, K.J. (ed.) TMS, 2001. pp. 527–533.

33. Westbrook, J.H. Precipitation of Ni_3Al from nickel solid solution as ogdoadically diced cubes, Z. *Kristallog.*, vol. 110, 1958, pp. 21–29.

34. Douglas, A., Neethling, J.H, Santamarta, R., Schryvers D. and Cornish, L.A. Unexpected ordering behaviour of Pt_3Al intermetallic precipitates, *J. Alloys and Compounds*, in press, vol. 432, 2007, pp. 96–102.

35. Porter, D.A. and Easterling, K.E., *Phase Transformations in Metals and Alloys*, Van Nostrand Reinhold Company, New York, 1981.

36. Sims, C.T., Stolof, N.S., and Hagel, W.C., *Superalloys II: High Temperature Materials for Aerospace and Industrial Power*, John Wiley and Sons, New York, 1987.

37. Süss, R., Hill, P.J., Ellis, P., and Wolff I.M. The oxidation resistance of Pt-base γ/γ' analogues to Ni-base superalloys, *Proc. 7th European Conference on Advanced Materials and Processes*, Rimini, Italy, 2001.

38. Wood, G.C., and Stott, F.H. Oxidation of alloys. *Mater. Sci. Technol.*, vol. 3, 1987. pp. 519–530.

39. Süss, R., Hill, P.J., Ellis, P. and Cornish, L.A. The oxidation resistance of Pt-Base superalloy Pt_{80}:Al_{14}:Cr_3:Ru_3 compared to that of Pt_{86}:Al_{10}:Cr_4 *Proc. Microsc. Soc. south. Afr.*, Johannesburg, 2001. vol. 31, p. 21.

40. Süss, R., Freund, D., Völkl, R., Fischer, B., Hill, P.J., Ellis, P., and Wolff, I.M. The creep properties of Pt-base γ/γ' analogues to Ni-base superalloys. *Mater. Sci. Eng. A*, vol. 338, 2002. pp. 133–141.

41. Cornish, L.A., Süss, R., Chown, L.H., Douglas, A,. Matema, M., Glaner, L. and Williams, G., New Pt-based alloys for high temperature application in

aggressive environments: *The next stage*, *Southern African Institute of Mining and Metallurgy conference 'Platinum Surges Ahead'*, Symposium series S45, Sun City, 8–12 October 2006. pp. 57–66.

42. CHOWN, L.H., CORNISH, L.A. and JOJA, B. Structure and properties of Pt-Al-Co alloys, *Proc. Microsc. Soc. south. Afr.*, Pretoria, 2004. vol. 34, p. 11.

43. GLANER, L., CORNISH, L.A. and JOJA, B. Investigation of the Ni-Pt-Ru phase diagram, *Proc. Microsc. Soc. south. Afr.*, Pretoria, 2004. vol. 34, p. 9.

44. NZULA, M. and CORNISH, L.A. Solidification and hardness studies in selected Cr-Ni-Pt alloys, *Proc. Microsc. Soc. south. Afr.*, Pietermaritzburg, 2005. vol. 35, p. 8.

45. SÜSS, R., CORNISH, L.A. and WITCOMBE, M.J. Investigation of as-cast alloys in the Pt-Cr-Ru system, *J. Alloys and Compounds*, 2006, vol. 416 (nos. 1–2), pp. 80–92.

46. SÜSS, R., CORNISH, L.A. and WITCOMBE, M.J. Investigation of isothermal sections at 1000°C and 600°C in the Pt-Cr-Ru system, submitted to *J. Alloys and Compounds.*

47. BIGGS, T., CORTIE, M.B., WITCOMBE, M.J. and CORNISH, L.A., Platinum Alloys for Shape Memory Applications, *Plt. Met. Rev.*, vol. 47, no. 4, 2003, pp. 142–156.

48. DOUGLAS, A., NEETHLING. J.H. and CORNISH, L.A., Dislocation distribution in a Pt-based analogue of Ni-Based superalloys, *Proc. Microsc. Soc. South. Afr.*, Pretoria, 2004. vol. 34, p. 12.

49. KERAAN, T. and LANG, C.I. High Temperature Investigation into Platinum-base Superalloys, *Proc. Microsc. Soc. South. Afr.*, Cape Town, 2003, vol. 32, p. 14.

50. KERAAN, T. and LANG, C.I. High Temperature Mechanical Properties and Behaviour of Platinumbase Superalloys for Ultra- high Temperature use, *African Materials Research Society Conference*, Johannesburg, 2003, pp. 154–155.

51. ASTM Standards, Standard Test Methods for Tension Testing of Metallic Metals, Designation E8-93, 1993, ASTM, pp. 130–149.

52. LUCAS, G.E., ODETTE, G.R., SOKOLOV, M., SPÄTIG, P., YAMAMOTO, T., and JUNG, P. Recent progress in small specimen test technology, *J.Nucl. Mater.*, 2002, vol. 307–311, pp. 1600–1608.

53. PANAYOTOU, N.F. The use of microhardness to determine the strengthening and microstructural alterations of 14 MeV neutron irradiated metals, *J. Nucl. Mater.*, 1982, vol. 108 and 109, pp. 456–462.

54. KOHYAMA, A., ASANO, K. and IGATA, N., Influence of radiation on materials properties : *15th International symposium (part II), ASTM-STP* 956, 1987, p. 111.

55. KOHNO, Y., KOHYAMA, A., HAMILTON, M.L., HIROSI. T., KATOH, Y. and GARNER, F.A. Specimen size effects on the tensile properties of JPCA and JFMS, *J. Nucl. Mater.*, 2000, vol. 283-287, pp. 1014–1017.

56. SÜSS, R., DOUGLAS, A., CORNISH, L.A., and JOJA, B. An Electron Microscope Investigation of Tensile Samples of Pt-Based Superalloys, *Proc. Microsc. Soc. south. Afr.*, Pretoria, 2004, vol. 34, p. 10.

57. SÜSS, R., CHOWN, L.H., DOUGLAS, A., and CORNISH, L.A. Experimental and Thermo-CalcTM work on the development of Pt-based superalloys, unpublished research, Mintek, Randburg, South Africa, October 2003.

58. SÜSS, R., CORNISH, L.A., CHOWN, L.H., and GLANER, L. Tensile Properties of Pt-based Superalloys, presented at *Beyond Ni-based Superalloys, TMS 2004 133rd Annual Meeting and Exhibition*, 269, Charlotte, North Carolina, USA, 14–17 March 2004. (Abstract)

59. Johnson-Matthey Internet URL: http:// www.platinum.matthey.com.

60. Dispersion-strengthened high-temperature materials, Brochure, Plansee.

61. PATHER, R., MITTEN, W.A., HOLDWAY, P., UBHI, H.S., and WISBEY, W.A. Effect of High Temperature Environment on High Strength Titanium Aluminide Alloy, *Proc. Advanced Materials and Processes for Gas Turbines*, TMS, 2003, pp. 309–316.

62. MACLACHLAN D.W. and KNOWLES, D.M. Modelling and prediction of the stress rupture behaviour of single crystal superalloys, *Mat. Sci. and Eng. A*, 2001, vol. 302, pp. 275–285.

63. VÖLKL, R., WENDEROTH, M., PREUSSNER, J., VORBERG, S., FISCHER, B., and GLATZEL, U. A review on the progress towards Pt-base superalloys for ultra high temperature applications, *Southern African Institute of Mining and Metallurgy conference 'Platinum Surges Ahead'*, Symposium series S45, Sun City, 8–12 October 2006. pp. 67–71.

64. ZHAO, J.-C., LACKSON, M.R., PELUSO, L.A., and BREWER, L., N. A Diffusion Multiple Approach for the Accelerated Design of Structural Materials, *MRS Bull.* 2002. pp. 324–329.

65. VORBERG, S., PhD thesis, Universität Bayreuth, 2006.

66. VÖLKL, R. and FISCHER, B. Mechanical Testing of Ultra-High Temperature Alloys. *Experimental Mechanics*, vol. 44, 2004, no. 2, pp. 121–127.

67. VORBERG, S., FISCHER, B., LUPTON, D., WENDEROTH, M., GLATZEL, U., and VÖLKL, R. Overview of the high-temperature mechanical properties of Pt-alloys, *Southern African Institute of Mining and Metallurgy conference 'Platinum Surges Ahead'*, Symposium series S45, Sun City, 8–12 October 2006. pp. 73–79.

68. WEERTMAN, J. *Trans. AIME*, vol. 216, 1969, p. 207 (cited by EVANS, R.W. and WILSHIRE, B., Introduction to Creep, Institute of Metals, 1993).

69. WEERTMAN, J. *Trans. Acta Metall.*, vol. 25, 1977, p. 1393 (cited by EVANS, R.W. and WILSHIRE, B., Introduction to Creep, Institute of Metals, 1993).

70. FISCHER, B. Reduction of Platinum Corrosion in Molten Glass, *Plat. Met. Rev.*, 1992, vol. 36, no. 1, pp. 14–25.

71. MALEDI, N.B., POTGIETER, J.H., SEPHTON, M., CORNISH, L. A,. CHOWN, L., and SÜSS, R. Hot, Corrosion Behaviour of Pt-alloys for Application in the Next Generation of Gas Turbines, *Southern African Institute of Mining and Metallurgy SAIMM conference 'Platinum Surges Ahead'*, Symposium series S45, Sun City, 8–12 October 2006. pp. 81–90.

72. ELLIOT, P., Practical Guide to High Temperature Alloys. Nickel Development Institute. 1990. pp. 1–10.

73. PRAKASH, G.S. and SINGH, S. Effects of MgO and CaO on hot corrosion of Fe base superalloy superfer 800H in Na_2SO_4-60%V_2O_5 environment, *British Corrosion Journal*, 2002, vol. 37, no. 1, pp. 56–62.

74. YOSHIBA, M. Effect of hot corrosion on the mechanical performances of superalloys and coatings systems, *Corrosion Science*, vol. 35, nos. 5–8. 1993. pp. 1115–1124. ◆